Life Sciences 216 (2019) 156–167

Contents lists available at ScienceDirect

Life Sciences

journal homepage: www.elsevier.com/locate/lifescie

CRTH2 antagonist, CT-133, effectively alleviates cigarette smoke-induced acute lung injury

Musaddique Hussain[a], Chengyun Xu[a], Minli Yao[a], Qin Zhang[a], Junsong Wu[b], Xiling Wu[c], Meiping Lu[c], Lanfang Tang[c], Fugen Wu[d,*], Ximei Wu[a,**]

[a] Department of Pharmacology, Zhejiang University, School of Medicine, Hangzhou City 310058, China
[b] Department of Critical Care Medicine and Orthopedics, The First Affiliated Hospital, Zhejiang University, School of Medicine, Hangzhou City 310009, China
[c] Department of Respiratory Medicine, the Affiliated Children Hospital, Zhejiang University School of Medicine, Hangzhou City 310052, China
[d] Department of Pediatrics, The First People's Hospital of Wenling City, Wenling City 317500, China

ARTICLE INFO

Keywords:
CRTH2 antagonist
PGD_2
Cigarette smoke
Pro-inflammatory mediators
RAW 264.7 macrophages

ABSTRACT

Aims: Acute lung injury (ALI) and acute respiratory distress syndrome (ARDS), characterized by overwhelming lung inflammation, are associated with high mortality. Cigarette smoke (CS) is one of the major causes of ALI/ARDS. Since high expression of prostaglandin (PG) D_2 has been observed in CS-induced lung injury. Currently, no effective pharmacological therapies are available to treat ALI, and supportive therapies remain the mainstay of treatment. Therefore, we investigated the protective effect of CT-133, a newly discovered selective CRTH2 antagonist, on CS-induced ALI in vivo and in vitro.

Main methods: CT-133 (10 and 30 mg/kg), dexamethasone (1 mg/kg) and normal saline were intratracheally administrated 1 hr prior to whole-body CS-exposure for seven consecutive days to study the key characteristics of ALI. Subsequently, CSE (4%)- and PGD_2-stimulated RAW 264.7 macrophages were used to evaluate the protective effect of CT-133.

Key findings: CT-133 remarkably attenuated infiltration of inflammatory cells, neutrophils, and macrophages in the BALF, albumin contents, expression of IL-1β, IL-6, TNF-α and KC, lung myeloperoxidase (MPO) activity and lung histopathological alterations caused by CS exposure in mice. Moreover, CT-133 not only reversed the uncontrolled secretion of IL-1β, IL-6, TNF-α and KC from CSE- and PGD_2-stimulated RAW 264.7 macrophages but also augmented IL-10 production in both in vivo and in vitro studies. Additionally, CT-133 alleviated in vitro neutrophil migration chemoattracted by PGD_2.

Significance: Our results provide the first evidence that targeting CRTH2 could be a new potential therapeutic option to treat CS-induced ALI.

1. Introduction

Acute lung injury (ALI) and its severe demonstration, acute respiratory distress syndrome (ARDS), are life-threatening clinical syndromes. The most characteristic pathological features of ALI/ARDS include increased pulmonary vascular permeability and edema, inappropriate recruitment of alveolar macrophages and pulmonary neutrophils, uncontrolled secretion of pro-inflammatory mediators, surfactant dysfunction, impaired gas exchange, and subsequent respiratory failure owing to progressive and refractory hypoxemia [1]. Despite decades of extensive research, ALI/ARDS remain a major cause of morbidity and mortality in critically ill patients, with 10% prevalence in intensive care units (ICU) and 40–46% mortality [2], and no definite pharmacological agent is available yet [3]. However, scarce pharmacological options for ALI present an unrelenting challenge in the field of drug development. Therefore, new therapeutic approaches are needed to improve the drug development for ALI.

Injurious effects of cigarette smoke (CS) on human health are progressively being acknowledged both in animal and human studies. CS is a highly complex mixture that contains substantive amounts of toxic oxidants, nitric oxide, organic compounds, free radicals and microbial cell components including bacterial lipopolysaccharide (LPS) [4]. CS increases susceptibility to the development of ALI/ARDS in critically ill patients [5–7]. CS exposure modifies the trafficking and function of

* Correspondence to: F. Wu, Department of Pediatrics, The First People's Hospital of Wenling City, 190 Taiping Southern Road, Wenling City 317500, China.
** Correspondence to: X. Wu, Department of Pharmacology, School of Medicine, Zhejiang University, 866 Yuhangtang Road, Hangzhou 310058, China.
E-mail addresses: 13600587789@163.com (F. Wu), xiwu@zju.edu.cn (X. Wu).

https://doi.org/10.1016/j.lfs.2018.11.039
Received 16 August 2018; Received in revised form 16 November 2018; Accepted 18 November 2018
Available online 22 November 2018

alveolar macrophages and pulmonary neutrophils [8,9], augments both lung epithelial and endothelial permeability [10,11], and encourages the production of pro-inflammatory cytokines and chemokine [12]; pathways central to the pathogenesis of ALI/ARDS. Nevertheless, CS exposure induces the pulmonary inflammation in animals that are appropriate for the pharmacological evaluation of novel therapeutics for ALI.

Prostaglandin (PG) D_2, primarily released from mast cells and to a lesser extent from antigen presenting cells and Th2 lymphocytes, exhibits a critical role in mediating airway inflammation, and exerts its assorted biological actions via D-type prostanoid receptor (DPs), namely DP_1 and DP_2; later known as chemoattractant receptor-homologous molecule expressed on Th2 cells (CRTH2) [13]. Particularly, CS increases the absolute number of mast cells in smokers [14,15], and PGD_2 is one of the predominant product released from CS-activated mast cells [16,17]. Elevated levels of PGD_2 [18,19] and CRTH2 [20] have been observed in CS-exposed in vivo studies, and a correlation has been noticed between PGD_2 concentrations in BALF and CS-induced disease severity [21]. Moreover, activated PGD_2/CRTH2 receptors on macrophages promoted the neutrophils recruitment and augmented the disease severity through excessive production of pro-inflammatory cytokines and consequent neutrophil activation [22] while CRTH2 antagonism inhibited the CS-induced inflammation [23,24]. The similar protective effect was shown after genetic deletion of CRTH2 [25]. However, these evidence prompted us to investigate the protective effect of a newly discovered CRTH2 antagonist, CT-133, against ALI using CS-induced ALI murine models and CSE-stimulated RAW 264.7 macrophages.CT-133 shows potential response against allergic asthma and rhinitis [26] but to our knowledge, no one has evaluated its protective effect against CS-induced ALI.

In this study we reported for the first time that specific inhibition of CRTH2 by CT-133 efficiently reduced the CS-induced lung injury most probably through attenuation of inappropriate infiltration of macrophages and neutrophils into alveolar spaces, pulmonary vascular permeability, and pro-inflammatory mediators production; suggesting that CRTH2 could be a new potential therapeutic target for appropriate therapy of CS-induced ALI.

2. Materials and methods

2.1. Compound

CT-133 ($C_{20}H_{19}FN_3NaO_4S$) is a newly developed, well tolerated, selective and potent CRTH2 receptor antagonist with 99.6% purity

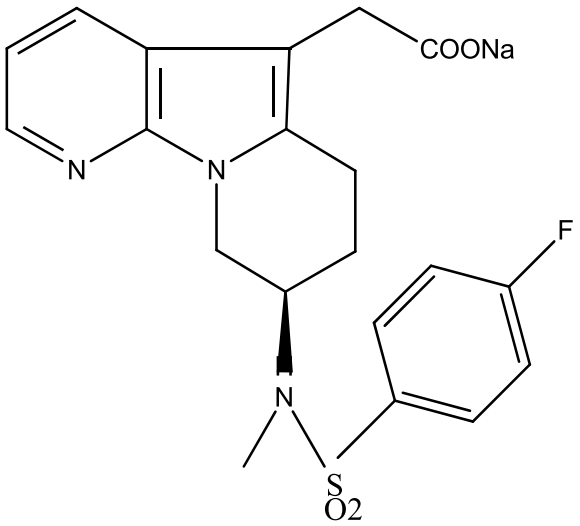

Fig. 1. Structure of CT-133.

Table 1
Inhibition rate (%) of CT-133 for CRTH2 receptor compared with other prostanoid receptors.

Receptors	$CRTH_2$	DP_1	TP	EP_1	EP_2	EP_3	EP_4	FP	IP
Inhibition rate (%)	100	−3	−1	−1	−6	11	−1	9	3

Abbreviations: TP, Thromboxane Receptor; EP_1, Prostaglandin E_2 receptor 1; EP_2, Prostaglandin E_2 receptor 2; EP_3, Prostaglandin E_2 receptor 3; EP_4, Prostaglandin E_2 receptor 4; FP, Prostaglandin F receptor; IP, Prostacyclin receptor.

(Fig. 1). Detailed in-vivo profile of CT-133 has been described [26]. Briefly, CT-133 demonstrated potent human CRTH2 inhibition with inhibitory constant (Ki) of 2.2 nM whereas inhibitory constant (Ki) for Human DP_1 was > 3800 nM. The average IC_{50} value for antagonism of PGD_2-induced eosinophil shape change in human was 1.0 nM. CT-133 antagonized PGD_2-mediated calcium mobilization in a concentration-dependent manner (IC_{50} = 17.1 nM). The average IC_{50} value for antagonism of PGD_2-induced cAMP accumulation in human was 22.9 nM. Moreover, inhibition rate (%) of CT-133 to CRTH2 and other prostaglandin receptors is depicted in Table 1. In addition, a single oral dose administration showed 89.6%, 85.4%, and 71.6% bioavailability in mice, dog, and rat respectively. Oral repeated administration in rats displayed no significant difference in AUCinf, $T_{1/2}$, Cmax, and Cmin between day one and day seven. The drug did not show any inducing effect on metabolic enzymes and established outstanding safety profile in preclinical studies. Single oral administration assay demonstrated no toxic effects in rat (300, 1000, 2000 mg/kg/day) and dog (100, 300, 1000 mg/kg/day; 100 mg/kg/day for seven-day).

2.2. Chemicals and reagents

All chemicals were of research grade. CT-133 was obtained from CSPC Pharmaceutical Group (Shijiazhuang City, China). Phosphate buffered saline (PBS), dexamethasone (Dex), and fetal bovine serum (FBS) were obtained from Sigma Chemical Co. (St. Louis, MO, USA). Penicillin/streptomycin was purchased from Thermo Fisher Scientific (Waltham, MA, USA). Myeloperoxidase (MPO) and albumin determination kits were taken from Jiancheng Bioengineering Institute of Nanjing (Nanjing, Jiangsu Province, China). ELISA kits of IL-β (batch # 2201B70832), IL-6 (batch # 220680333), TNF-α (batch #A28280643), and IL-10 (batch #A21080834) were procured from Multi-sciences (LIANKE) Biotech Ltd. (Hangzhou, China) while keratinocyte chemoattractant (KC; mouse homologue of IL-8) ELISA kit (batch # 20180717) was obtained from 4A Biotech Co. Ltd. (Beijing, China). Prostaglandin D_2 (PGD_2) and PGD_2 ELISA kit (batch # 0492341) were purchased from Cayman chemical (Michigan, USA). PCR primers for IL-β, IL-6, TNF-α, KC, IL-10, and β-actin were bought from Shanghai Bioengineering Ltd. (Shanghai, China). RNAiso plus was obtained from Takara Bio Inc. (Otsu, Shiga, Japan). HiScript 5 × Q RT Super Mix, including dNTP, buffer, HiScript reverse transcriptase, random primers/Oligo dT primer mix and RNase inhibitor, and SYBR-Green master mix were bought from Vazyme Biotech, Ltd. Nanjing, China. Boyden chamber assay kits were purchased from Cell Biolabs, Inc. (San Diego, CA, USA). RPMI-1640 medium were purchased from GE Healthcare Life Sciences (HyClone Laboratories, Utah, USA).

2.3. Mice handling

Specific pathogen-free (SPF) female Balb/c mice (22–28 g; 8 weeks old) were purchased from Shanghai SIPPR-BK Laboratory Animals Co. Ltd. Shanghai, China (certificate No. SCK (hu) 2013–0016 and 2008001648391). Mice were kept in isolated ventilated cages (4–5 mice/cage) under controlled environmental condition (40–60% humidity; 24 ± 2 °C) with 12 h/12 h dark-light cycle and had free access

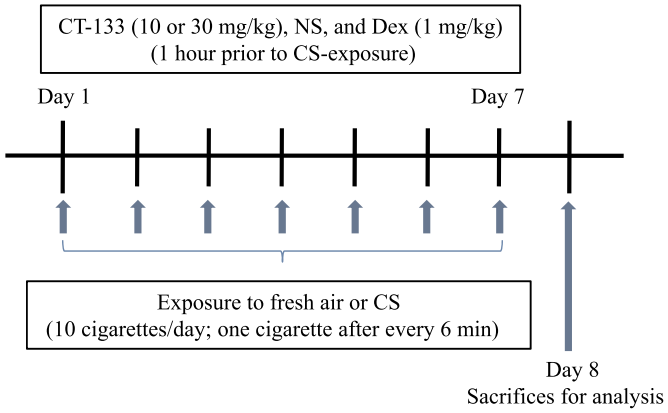

Fig. 2. A schematic sketch of the experimental procedure. The mice were whole-body exposed to fresh air or the mainstream cigarette smoke (CS) generated from 3R4F research grade; 10 cigarettes a day (one cigarette after every 6 min) for seven consecutive days. One hour prior to cigarette smoke, mice were subjected to intratracheal instillation of normal saline, Dex (1 mg/kg) and CT-133 (10 or 30 mg/kg). On day 8 (24 h after the last CS-exposure), mice were sacrificed to collect BALF and lung tissues for other analyses.

to regular rodent chow and distilled water. Ethical Committee of Zhejiang University, School of Medicine (Permit No. ZJU20170013) approved all of the mice handlings, procedures and experiments conducted in this study.

2.4. Cigarette smoke (CS)-induced lung injury models preparation and measurement of partial pressure of oxygen

CS-induced lung injury models were generated by following the previously described procedure [27]. Mice were randomly divided in five groups (12 in each): control/fresh air exposed, vehicle (NS) + CS-exposed, Dex (1 mg/kg) + CS-exposed, and CT-133 (10 and 30 mg/kg) + CS-exposed respectively, and were subjected to intratracheal instillation of normal saline, Dex (1 mg/kg) and CT-133 (10 or 30 mg/kg) for 1 h. After that, mice were exposed to mainstream cigarette smoke generated from 3R4F research grade cigarettes (containing approximately 600 mg TPM/m^3 and 29.9 mg nicotine/m^3) in a square plastic box (65 × 50 × 45 cm) once a day (10 cigarettes a day; one cigarette after every 6 min) for 7 consecutive days (Fig. 2). Mice were checked daily for their body weight and general condition. Twenty-four hours after last CS exposure, moor VMS-OXY™ monitor (Moor Instruments, United Kingdom) was used to measure the partial pressure of oxygen (PO_2) of all mice that measures oxygenated/deoxygenated hemoglobin concentration and oxygen saturation (percentage) in the microcirculation at the wavelength range of 500 to 650 nm. Afterward, all mice were euthanized to collect the broncho-alveolar lavage fluid (BALF) in order to measure inflammatory cells count, cytokines levels and albumin concentration, and lungs were harvested for determination of lung weight coefficient, histological examination and MPO activity.

2.5. Inflammatory cells counting

Mice were killed to surgically expose the trachea, and then right lungs were lavaged with 0.4 ml/time of sterilized normal saline containing 1% FBS and 5000 IU/L heparin three times to collect the BALF via tracheal tube. After measuring the total number of cells in BALF with a hemocytometer, remainder BALF was centrifuged immediately at 1000 ×*g* at 4 °C for 10 min. The supernatant was aliquoted and stored at −80 °C until measurement of cytokines or albumin concentration. Obtained cell pellets were smeared on slides. Afterward, Wright-Giemsa staining of prepared smears was performed to count 200 cells under a light microscope according to the morphological criteria of neutrophil, macrophage, and lymphocyte.

2.6. Lung weight ratio

As an index of pulmonary edema, lung weight ratio was measured by dividing the individual lung weight of each mouse, after aspirating the surface blood lung tissues, by its total body weight.

2.7. Albumin assay

Albumin determination kits were used to assess the albumin concentration in BALF supernatants with a spectrophotometer at 628 nm. Albumin concentrations ratio assessed from BALF represent not only the effused albumin level but also the pulmonary microvascular permeability.

2.8. In vivo cytokines assay via ELISA

Expression levels of pro-inflammatory cytokines (TNF-α, IL-β, IL-6), chemokine (KC) and anti-inflammatory cytokine (IL-10) in the supernatants of BALF were determined using respective ELISA determination kits according to the manufacturer's instructions. After measuring the optical density at 450 nm, expression of cytokines was calculated via standard curves.

2.9. Pulmonary histopathology

For histopathological examination, lower lobe of the left lung of each mouse was preserved in 10% neutral formalin. Preserved lobes were embedded in paraffin and then sectioned (4 μm) to expose the maximum longitudinal view of the main intrapulmonary bronchus. Hematoxylin and eosin (H&E) staining was performed using a standard protocol. Afterward, the 5-point scoring system was used to access the lung edema, severity of inflammation, and infiltration of inflammatory cells [28]. Briefly, the scoring system was, 0 = normal; 1 = very mild; 2 = mild; 3 = moderate; 4 = marked; 5 = severe inflammation. Scoring was performed in at least three different fields for each lung section. Mean scores were derived from 12 animals.

2.10. MPO assay

For the assessment of MPO activity, 50 mg strips of left lung tissue were washed and then homogenized with normal saline. Afterward, MPO activity was determined by measuring the changes in absorbance at 460 nm using MPO determination kits in accordance with the manufacturer's protocol.

2.11. Isolation of neutrophils and assessment of the effect of CT-133 on PGD2-induced neutrophils migration

Glycogen (1.5%) at the dose range of 20 ml/kg of body weight was injected intragastrically to mice. Four hours later mice were euthanized to isolate the neutrophils from peritoneal lavage [29]. The effect of CT-133 on neutrophils migration was assessed by using Boyden chamber assay kit (3 μm pore size), and PGD_2 was used as chemoattractant because activated PGD_2/CRTH2 receptors promote neutrophils migration [22,31]. Initially, isolated neutrophils (4×10^5) diluted in 100 μl HBSS were allowed to migrate toward PGD_2 (0.1, 1 and 10 μM) for 4 h in order to find out the suitable PGD_2 concentration. Later, isolated neutrophils (4×10^5) were pretreated with CT-133 (1 and 10 μM) and their migration toward PGD_2 (1 μM) was evaluated by counting the migrated neutrophils. Moreover, we also used another potent CRTH2 inhibitor, OC459, to countercheck the outcomes of CT-133.

Table 2
Primers used for quantitative RT-PCR.

Genes (Accession no.)	Primer sequences (5′ – 3′) (bp)	Product Length	Amplification profile (temp. (°C)/time (*sec.*))			Cycles (n)
			Denaturation	Annealing	Elongation	
IL-6 (NM_031168)	F: TGCCTTCTTGGGACTGAT R: TTGCCATTGCACAACTCTTT	183	95/10	58/30	72/30	40
TNF-α (NM_013693)	F: CCAGACCCTCACACTCAGAT R: GACAAGGTACAACCCATCG	187	95/10	58/30	72/30	40
IL-1β (NM_008361)	F: GTTCCCATTAGACAACTGC R: GATTCTTTCCTTTGAGGC	199	95/10	58/30	72/30	40
KC (NM_011339)	F:CAATGAGCTGCGCTGTCAGTG R: CTTGGGGACACCTTTTAGCATC	203	95/10	58/30	72/30	40
IL-10 (NM_010548.2)	F: TCAAGGCGCATGTGAACTCC R: GATGTCAAACTCACTCATGGCT	176	95/10	58/30	72/30	40
β-actin (NM_007393)	F: CACGATGGAGGGGCCGGACTCATC R:TAAAGACCTCTATGCCAACACAGT	214	95/10	58/30	72/30	40

2.12. Preparations of cigarette smoke extract (CSE)

CSE was prepared by following the previously described method [32]. In brief, mainstream smoke, generated from 3R4F research grade cigarettes, was passed through 50 ml of PBS by a vacuum pump. Five cigarettes were used for 50 ml of PBS, and each cigarette was lit for 5 min. A similar procedure was adopted for control solution preparation in the absence of cigarettes. After extraction, CSE was stored at −80 °C.

2.13. Isolation of primary macrophages and assessment of CSE-induced secretion of PGD_2 from primary macrophages

Primary macrophages were isolated from the peritoneal cavity by slightly modifying the previously described procedure [33]. In brief, thioglycollate (4%) at the dose range of 20 ml/kg of body weight was injected into the peritoneal cavity of mice for three consecutive days. On the 5th day (48 h after last thioglycollate injection), mice were euthanized to isolate the primary macrophages from peritoneal lavage. Isolate primary macrophages (4×10^5/well) were added to 12-well plates and allowed to culture at 37 °C. Afterward, the culture medium of 12-well plates was replaced with a serum-free RPMI-1640 medium for 10–12 h and then exposed to different concentrations of CSE (2%, 4%, and 8%) for 24. After treatment, the supernatants of the primary macrophages were harvested to measure the protein level of PGD_2 secreted extracellular using ELISA kit according to the manufacturer's instructions.

2.14. Cell viability assay

RAW 264.7 macrophage, mouse leukemic monocyte macrophage, cell line was purchased from American Type Culture Collection (ATCC, Manassas, VA, USA). RAW 264.7 macrophage was cultured in RPMI-1640 medium containing 10% FBS in the presence of penicillin (100 U/ml) and streptomycin (100 μg/ml). The cytotoxicity of CT-133 (0–100 μM) alone and in a combination of PGD_2 (0–100 μM) and CSE (1–10%) on RAW 264.7 macrophage was assessed using a methylthiazol-tetrazolium (MTT) assay in accordance with the manufacturer's protocol. Briefly, RAW 264.7 macrophages were plated at a concentration of 4×10^5 cells/ml in 96-well plates for 24 h and subsequently exposed to CT-133 (0–100 μM) for 1 h at 37 °C. Next, RAW 264.7 macrophages were further exposed to CSE (4%) and PGD_2 (10 μM) for 24 h, followed by treatment with MTT (5 mg/ml) for an additional 4 h at 37 °C. Then, the supernatant of each well was replaced with DMSO (200 μl/well) and absorbance was measured at 570 nm.

2.15. In vitro cytokines assay via ELISA and Real-time polymerase chain reaction (RT-PCR)

For ELISA and RT-PCR, RAW 264.7 macrophages were acclimated to two 12-well plates. After that, the culture medium of 12-well plates was replaced with a serum-free RPMI-1640 medium for 10–12 h and then exposed to CT-133 (10 and 100 μM) for 1 h. One hour later, one 12-well plate was treated with CSE (4%) and other with PGD_2 (10 μM) for 24 h. After treatment, the supernatant of treated cells was harvested to measure the protein levels of TNF-α, IL-1β, IL-6, KC, and IL-10 secreted extracellular using ELISA kits according to the manufacturer's instructions. Subsequently, RNA samples from each treated plates were extracted and reverse-transcripted into cDNA with HiScript 5 × Q RT SuperMix, and then subjected to RT-PCR. RT-PCR was performed with the BioRad CFX96 Touch™ Real-Time PCR Detection System (BioRad, USA) using AceQ® qPCR SYBR Green Master Mix, and threshold cycle numbers were obtained using BioRad CFX Manager Software. The primers used for RT-PCR reaction are depicted in Table 2. The housekeeping gene, β-actin, was used as an internal control. RT-PCR reactions were triplicated and the relative expression of the target mRNA was normalized by the respective β-actin.

2.16. Statistics

Numerical data were expressed as means ± SEM, and statistical calculations were performed using SPSS (SPSS Inc., Chicago, IL). One-way ANOVA was applied to compare the F values, if $p > 0.05$, Dunnett multiple comparisons tests were used for calculating the difference of parametric data; if $p < 0.05$, Mann-Whitney U non-parametric test was used to compare the difference. $p < 0.05$ and $p < 0.01$ were considered to be statistically significant.

3. Results

3.1. Effect of CT-133 on CS-induced inflammatory cells count in BALF

Twenty-four hours after last CS-exposure, the effect of CT-133 on the infiltration of total cells and differential cells, particularly neutrophils and macrophages, in BALF was analyzed via Wright–Giemsa staining method. As shown in Fig. 3A and B, the number of total cells, macrophages and neutrophils were prominently increased after CS-exposure ($p < 0.01$). Meanwhile, pretreatment with CT-133 (10 and 30 mg/kg) and Dex (1 mg/kg) significantly decreased the total cells, macrophages and neutrophils ($p < 0.01$). These significant effects demonstrate that CT-133 could considerably ameliorate CS-induced pulmonary inflammation via CRTH2 antagonism.

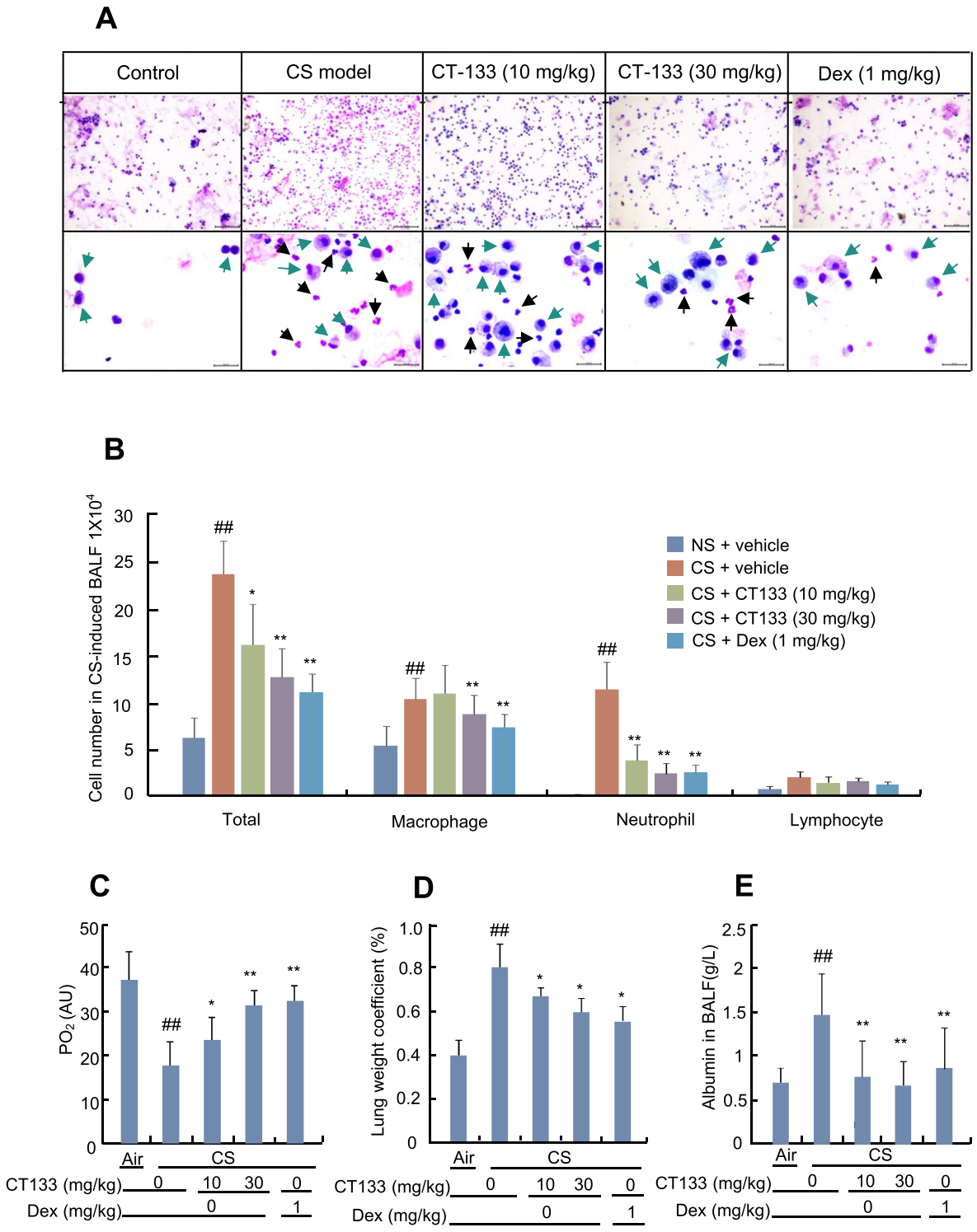

Fig. 3. Effect of CT-133on inflammatory cells count in BALF, partial pressure of oxygen (PO_2), lung weight coefficient and albumin contents in BALF. CT-133 (10 and 30 mg/kg), normal saline and Dex (1 mg/kg) were orally administrated 1 h prior to whole-body cigarette smoke-exposure for seven consecutive days. BALF was collected 24 h after the last CS-exposure. (A) The image of neutrophils (black arrowheads) and macrophages (green arrowheads) in collected BALF. (B) Infiltration profiles of the total cells, macrophages, neutrophils, and lymphocytes in the BALF. (C) The partial pressure of oxygen (PO_2) of all mice was measured by using the moor VMS-OXY™ monitor (Moor Instruments, United Kingdom) 24 h after CS-exposure. (D) After aspirating the surface blood from dissected lung tissues, lung weight coefficient was measured by dividing the individual lung weight of each mouse by its total body weight. (E) Albumin concentration in BALF was measured using albumin determination kits. $^{\#\#}p < 0.01$ versus control (Ctrl) group; $^{*}p < 0.05$ and $^{**}p < 0.01$versus model group. Values are expressed as mean ± SEM; $n = 12$ (each group). (For interpretation of the references to colour in this figure legend, the reader is referred to the web version of this article.)

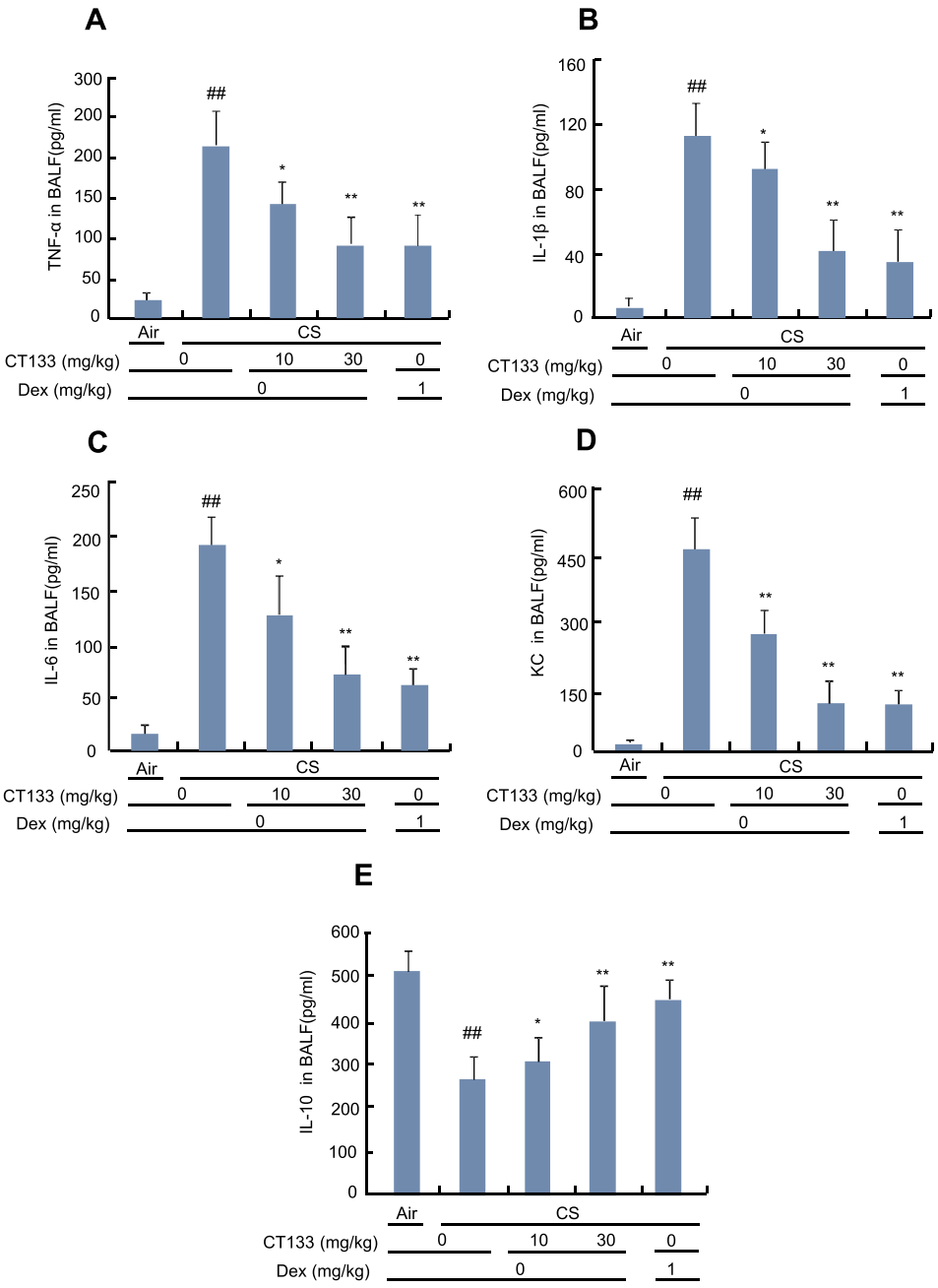

Fig. 4. Effect of CT-133 on the expression of pro-inflammatory cytokines (TNF-α, IL-β, IL-6), chemokine (KC) and anti-inflammatory cytokine (IL-10) in the BALF of CS-induced ALI mice. Collected BALF was subjected to analyze the expression levels of TNF-α (A), IL-β (B), IL-6 (C), KC (D) and IL-10 (E) by their respective ELISA kits. $^{\#\#}p < 0.01$ versus control (Ctrl) group; $^{*}p < 0.05$ and $^{**}p < 0.01$versus model group. Values are expressed as mean ± SEM; $n = 12$. (each group).

3.2. Effect of CT-133 on CS-induced hypoxemia, pulmonary edema, and lung permeability

CS-induced hypoxemia, pulmonary edema, lung permeability were assessed by measuring the partial pressure of oxygen (PO_2), lung weight coefficient, and BALF albumin contents respectively. In CS-treated groups, PO_2 was evidently decreased ($p < 0.01$) while lung weight coefficient and BALF albumin contents were strikingly augmented ($p < 0.01$) as compared to control group, telling that CS-induced animal models were successful. However, CT-133 (10 and 30 mg/kg) significantly elevated the PO_2 ($p < 0.01$) (Fig. 3C), partially decreased lung weight coefficient ($p < 0.05$) (Fig. 3D), and remarkably attenuated the BALF albumin contents ($p < 0.01$) (Fig. 3E). These excellent outcomes demonstrate that CRTH2 antagonism with CT-133 could effectively protect mice from CS-induced lung injury via mitigating the hypoxemia, pulmonary permeability, and edema.

3.3. Effect of CT-133 on CS-induced cytokines secretion in BALF

To determine whether CT-133 could affect the secretion of cytokines in BALF, expression levels of pro-inflammatory cytokines (TNF-α, IL-β, IL-6), chemokine (KC) and anti-inflammatory cytokine (IL-10) were detected using respective ELISA kits. As shown in Fig. 4 A, B, C and D, expression levels of TNF-α, IL-1β, IL-6, and KC were remarkably augmented in the CS-exposed group compared with the control group ($p < 0.01$). Meanwhile, CS-induced overexpression of TNF-α, IL-1β, IL-6, and KC were effectively reduced by CT-133 treatment (10 and 30 mg/kg) ($p < 0.01$). In contrast, the expression level of IL-10 was

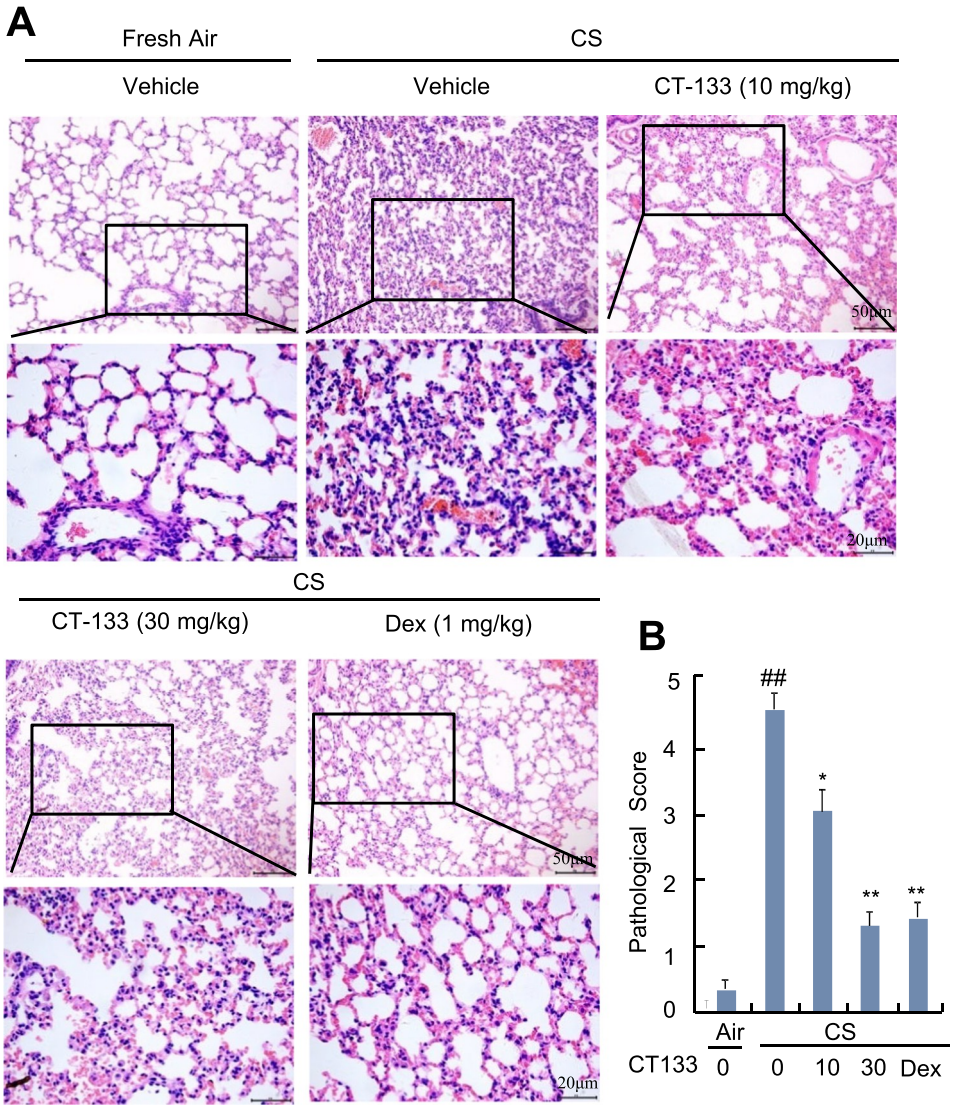

Fig. 5. Effect of CT-133 on histopathological changes in the lung tissues of CS-induced ALI mice. Hematoxylin-eosin staining of paraffin-embedded lung sections from each experimental group was performed for histopathological evaluation. (A) Representative images of lung tissues stained with H&E to demonstrate infiltration of macrophages, neutrophils, and inflammatory cells. (B) Quantitative analysis of infiltration of inflammatory cells and severity of inflammation was assessed from the lung sections. $^{\#\#}p < 0.01$ versus control (Ctrl) group; $^{*}p < 0.05$ and $^{**}p < 0.01$versus model group. Values are expressed as mean ± SEM; $n = 12$ (each group).

strikingly decreased in the CS-exposed group ($p < 0.01$) while CT-133 treatment reversed the CS-induced inhibition of IL-10 ($p < 0.01$) (Fig. 4E). These results indicate that blockade of CRTH2 receptors by CT-133 protects the CS-induced ALI mice from further pulmonary inflammation by inhibiting the production of pro-inflammatory cytokines and neutrophils chemokine and stimulating the production of an anti-inflammatory cytokine (IL-10).

3.4. Effect of CT-133 on CS-induced pulmonary histopathologic alterations

To evaluate the protective effect of CT-133 on CS-induced pulmonary histopathologic changes, H&E staining was performed. As shown in Fig. 5A, lung tissues of the control group showed normal pulmonary histology whereas CS-exposed lung tissues showed marked histopathologic changes, such as infiltration of inflammatory cells, macrophage, and neutrophils into alveolar spaces, and interstitial edema. Conversely, these changes were strikingly improved by pre-treatment with CT-133 (10 and 30 mg/kg) or Dex (1 mg/kg). Additionally, pathological scores were also assessed to find out the severity of inflammation, infiltration of inflammatory cells and lung edema. The results of pulmonary inflammatory scores showed that CS-exposure significantly increased mean pathological score ($p < 0.01$) while CT-133 (10 and 30 mg/kg) and Dex (1 mg/kg) considerably reduced the mean pathological scores in a dose-dependent manner ($p < 0.01$) (Fig. 5B). Compiled results imply that CT-133 markedly reduces the severity of CS-induced lung injuries by blockage of the CRTH2 receptor.

3.5. Effect of CT-133 on CS-induced MPO activity

Owing to promising protective outcomes, we further assessed the MPO activity of lung tissues. MPO, produced by activated neutrophils, acts as an important marker of neutrophils infiltration and lung tissue damage. We find that MPO activity of CS-exposed lung tissues was significantly increased as compared to fresh air-exposed ($p < 0.01$) (Fig. 6A). Noteworthy, CT-133 (10 and 30 mg/kg) and Dex (1 mg/kg) diminished the MPO activity ($p < 0.01$), demonstrating that CRTH2 receptor blockade efficiently inhibits the neutrophils infiltration into the alveolar and interstitial spaces.

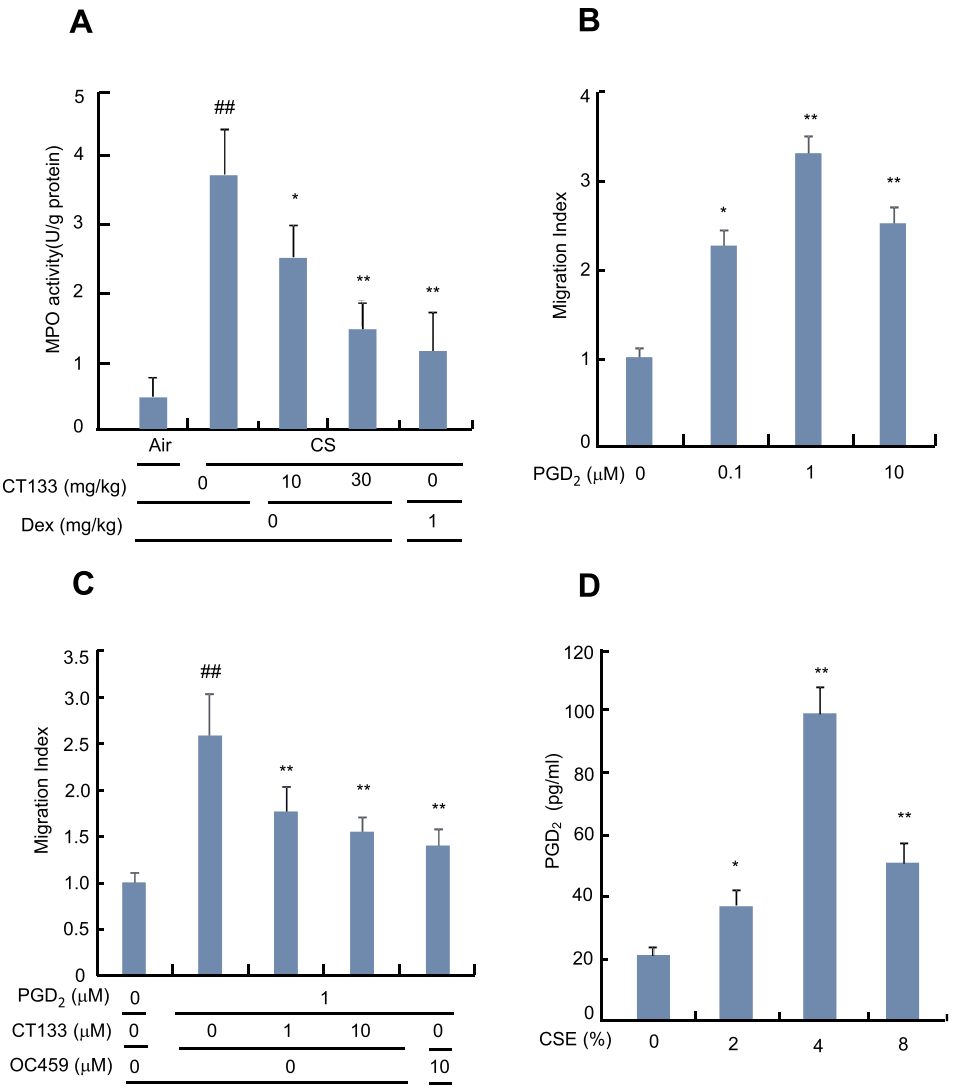

Fig. 6. Effect of CT-133on lung MPO activity and PGD_2-induced neutrophils migration in vitro, and assessment of CSE-induced secretion of PGD_2 from primary macrophages. (A) MPO activity from lung homogenates was measured using MPO kits. Values are expressed as mean ± SEM; $n = 12$ (each group). PGD_2-induced neutrophils migration was evaluated in the absence (B) and presence (C) of CT-133 using Boyden chamber assay kits (3 μm pore size). (D) Supernatants collected from isolated primary macrophages, pretreated with different concentrations of CSE (2%, 4%, and 8%) for 24 h, were harvested to measure the protein levels of PGD_2 using PGD_2 ELISA kit. $^{\#\#}p < 0.01$ versus control (Ctrl) group; $^{*}p < 0.05$ and $^{**}p < 0.01$versus PGD_2. All experiments were performed in triplicate wells for each condition and repeated at least thrice. Values are expressed as mean ± SEM.

3.6. Effect of CT-133 on PGD_2-induced neutrophils migration in vitro

Prompted by significant MPO outcomes, we further assessed the direct effect of CT-133 on PGD_2-induced neutrophils migration using Boyden chamber assay kit because activated PGD_2/CRTH2 receptors promote the neutrophils migration and its functioning [22,31]. Moreover, deleterious inflammatory mediators released by neutrophils mostly worse the lung injury. Neutrophils were isolated from mice abdominal cavities after challenge with 1.5% glycogen and then subjected to Wright-Giemsa staining and cell viability assay to inspect the characteristics of neutrophils (data not shown). Four hours of incubation showed significant neutrophils migration ($p < 0.01$) toward PGD_2 (1 and 10 μM) (Fig. 6B). Meanwhile, pretreatment with CT-133 (1 and 10 μM) significantly attenuated PGD_2-induced neutrophil migration ($p < 0.01$) (Fig. 6C). Likewise, OC459, another CRTH2 antagonist, also suppressed the PGD_2-induced neutrophils migration (Fig. 6C). Taken together, these data clearly imply that CRTH2 antagonists appreciably reduce the PGD_2-induced neutrophils migration.

3.7. CSE promotes the secretion of PGD_2 from primary macrophages

To access whether CSE exhibit impact on PGD_2 secretion, we treated the isolated primary macrophages with different concentration of CSE (2%, 4%, and 8%) for 24 h, and then evaluated the protein levels of extracellular secreted PGD_2 via PGD_2 ELISA kit. We found that CSE (4%) treatment significantly promoted the secretion of PGD_2 from primary macrophages as compared to control ($p < 0.01$) (Fig. 6D).

3.8. Effect of CT-133 on CSE- and PGD_2-induced cytokines secretion from RAW 264.7 macrophages

Based on remarkable in vivo outcomes, we further considered whether CT-133 treatment could inhibit the secretion of cytokines from CSE- and PGD_2-stimulated RAW 264.7 macrophages because activated PGD_2/CRTH2 receptors on macrophages markedly augment disease activity via increased expression of pro-inflammatory cytokines [22]. MTT assay revealed that PGD_2 (10 μM) plus CT-133 up to100 μM, and CSE 4% plus CT-133 up to100 μM were not toxic to RAW 264.7 macrophages (data not shown). Moreover, ELISA (Fig. 7) and RT-PCR (Fig. 8) results demonstrated that CT-133 (10 and 100 μM) treatment not only suppressed the protein and mRNA levels of IL-1β, IL-6, TNF-α, and KC produced from CSE- and PGD_2-stimulated RAW 264.7 macrophages ($p < 0.01$) but also reversed the CSE- and PGD_2 induced inhibition of IL-10 ($p < 0.01$) in a dose-dependent manner. Hence, obtained in vitro (Figs. 7 and 8) results were similar to in vivo (Fig. 4) results. Collectively these data suggest that CRTH2 antagonism effectively ameliorates the pro-inflammatory cytokines and chemokines production and promotes the anti-inflammatory cytokine production from CSE- and PGD_2-activated RAW 264.7 macrophages.

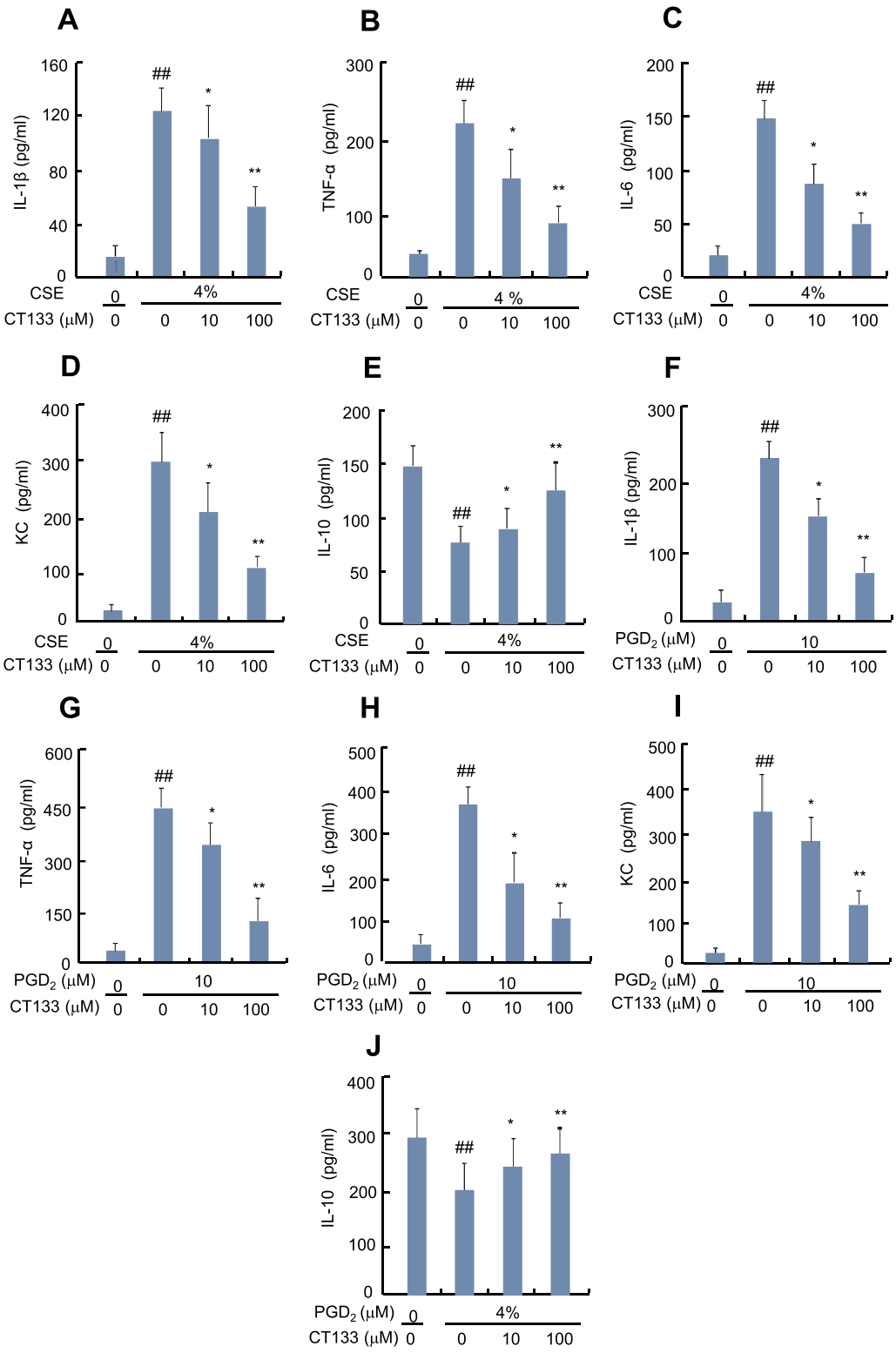

Fig. 7. Effect of CT-133 on CSE (4%)- and PGD_2-induced protein levels of pro-inflammatory cytokines (TNF-α, IL-β, IL-6), chemokine (KC) and anti-inflammatory cytokine (IL-10) from RAW 264.7 macrophages. Supernatants collected from RAW 264.7 macrophages, pretreated with CT-133 for 1 h and CSE/PGD_2 for 24 h, were harvested to measure the protein levels of IL-β (A and F), TNF-α (B and G), IL-6 (C and H), KC (D and I) and IL-10 (E and J) secreted extracellular using ELISA kits according to the manufacturer's instructions. $^{\#\#}p < 0.01$ versus control (Ctrl) group; $^{*}p < 0.05$, and $^{**}p < 0.01$versus PGD_2. All experiments were performed in triplicate wells for each condition and repeated at least thrice. Values are expressed as mean ± SEM.

4. Discussion

Cigarette smoke is the major leading cause of morbidity and mortality in the world, and has been reported as a single greatest preventable cause of death in developed countries. In this study, we explored the protective effect of CT-133, a newly discovered potent CRTH2 antagonist, on acute lung injury using CS-induced ALI murine models, and CSE-stimulated RAW 264.7 macrophages.

Accumulated epidemiological evidence has revealed that both active and passive CS exposure enhance vulnerability to ALI/ARDS development [5,7]. Excessive influx of inflammatory cells, particularly macrophages and neutrophils, is an important pathological hallmark of CS-induced ALI [8,12,34,35]. Under physiological conditions, quick and appropriate macrophage and neutrophil infiltration are imperative for clearance of alveolar debris and pathogens, while CS hinders the phagocytic abilities of macrophage [36,37] and neutrophils [38] as well

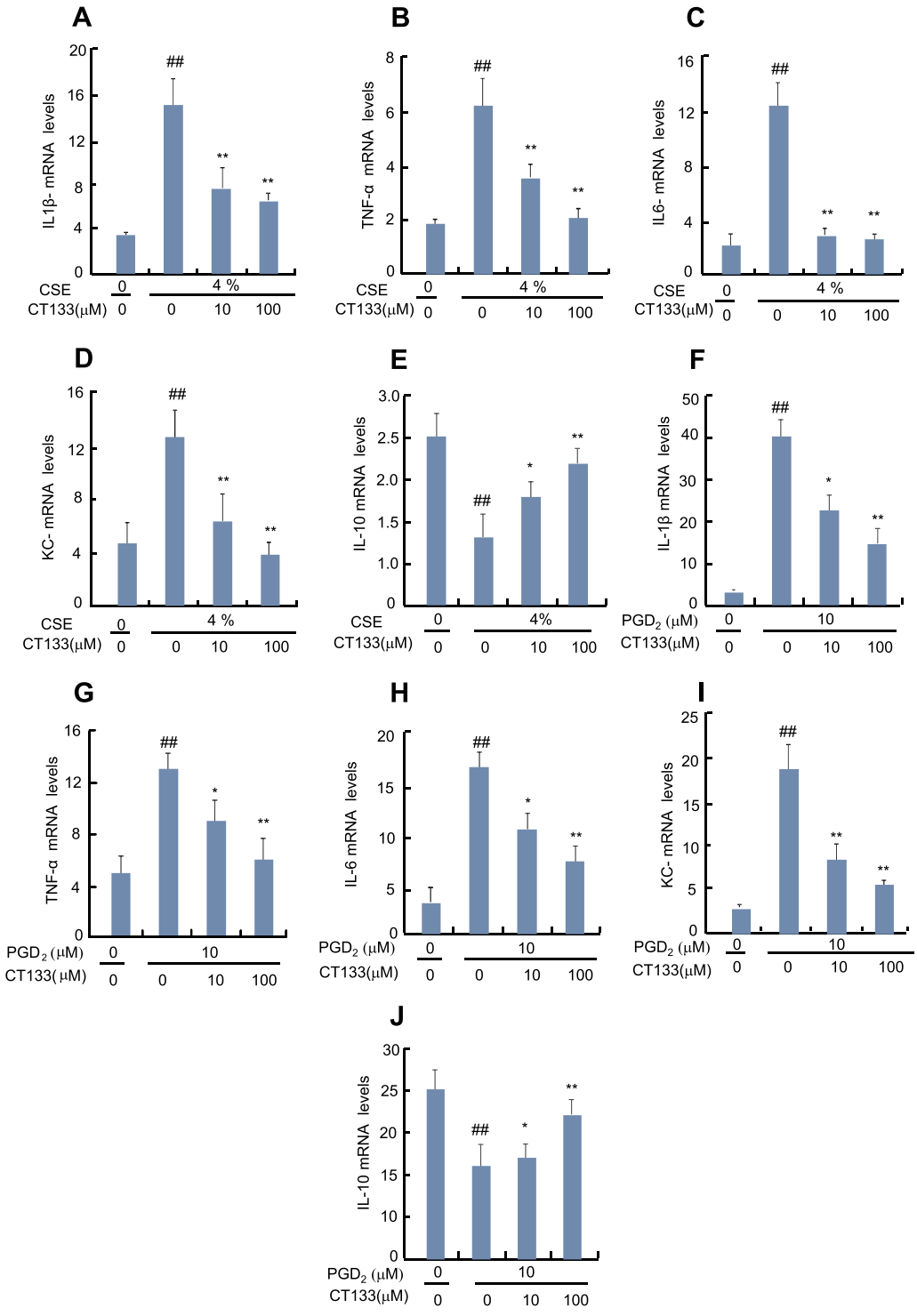

Fig. 8. Effect of CT-133 on CSE (4%)- and PGD_2-induced mRNA expression of pro-inflammatory cytokines (TNF-α, IL-β, IL-6), chemokine (KC) and anti-inflammatory cytokine (IL-10) from RAW 264.7 macrophages. Total RNAs extracted from RAW 264.7 macrophages, pretreated with CT-133 for 1 h, and CSE/PGD_2 for 24 h, were subjected to analyze the mRNA expression levels of IL-β (A and F), TNF-α (B and G), IL-6 (C and H), KC (D and I) and IL-10 (E and J) using RT-PCR respectively. $^{\#\#}p < 0.01$ versus control (Ctrl) group; $^{*}p < 0.05$ and $^{**}p < 0.01$versus PGD_2. All experiments were performed in triplicate wells for each condition and repeated at least thrice. Values are expressed as mean ± SEM.

as disrupts the pulmonary vascular permeability [11,39,40]. Importantly, PGD_2, released from CS-activated mast cells [16,17], was found to be involved in arbitrating macrophage migration in CS-induced lung injury models [23] and activated PGD_2/CRTH2 receptors on macrophages orchestrate neutrophils recruitment into the lung [22]. Furthermore, CRTH2 exhibits an important role in neutrophil migration [31] because CRTH2 agonist elicits the neutrophil migration [41], while CRTH2 antagonism [42] or genetic deletion of the CRTH2 receptor [31] improved the impaired neutrophil trafficking into the lung. Importantly, neutrophil infiltration and its activation in lung led to structural changes and bronchial inflammation [43,44]. Hence, many studies have been focused on controlling neutrophilic inflammation in CS-induced lung injury [23,45,46]. Consistent with previous studies, our results demonstrated that CT-133 dose-dependently and significantly attenuated CS-induced inflammatory cells, macrophage and neutrophils count in BALF and ameliorated lung MPO activity. In addition, lung histological examination and lung injury score also proved that CT-133 evidently attenuated the severity of inflammation and infiltration of inflammatory cells. Collected outcomes suggest that protective effects of CT-133 might be due to attenuation of pulmonary vascular permeability and inhibition of neutrophils migration because our further investigations revealed that CT-133 strikingly minimized

CS-induced BALF albumin contents and lung weight coefficient, and blocked PGD_2-induced in vitro neutrophils migration.

Of note, CS-associated lung injury is closely linked with augmented influx of macrophages that subsequently intensify the lung injury [34,47] while macrophage depletion alleviates CS-induced pulmonary inflammation via reducing cytokines and chemokine production in BALF [48]. Similar effect has been observed from PGD_2/CRTH2 activated macrophages in LPS-induced ALI models [22] while the genetic deletion of CRTH2 reduced the production of TNF-α in sepsis, a common cause of ALI [31]. Nevertheless, macrophage-derived TNF-α [49,50] and IL-1β [51], early response cytokines to lung injury, stimulate the production of IL-6 [52] and IL-8 [53]. Released pro-inflammatory cytokine (TNF-α, IL-1β, IL-6) [54,55] particularly IL-8 [56,57] triggers the inappropriate neutrophils migration across the endothelial barrier, that eventually exaggerates the lung injury, while genetic ablation of CXCR2, IL-8 receptor beta, showed protective response against CS-induced lung injury [58]. Notably, elevated expression levels of TNF-α, IL-1β, IL-6, and IL-8 have been observed in various CS-induced in vivo and in vitro lung injury models [59–63] while inhibition of pro-inflammatory cytokines and chemokines production proved effective in CS-induced lung injury [64,65]. Moreover, IL-10 has been reported as a potent immunomodulatory cytokine in counterbalancing the pro-inflammatory response. Decreased IL-10 level has been observed in ALI mice [66] while IL-10 treatment attenuated the severity of ALI [67]. Consistent with previous studies, we observed augmented infiltration of macrophages in BALF, overexpression of pro-inflammatory cytokines and chemokines and decreased expression of IL-10 while CRTH2 antagonism with CT-133 altered the inappropriate recruitment of alveolar macrophages, alleviated the uncontrolled overexpression of pro-inflammatory cytokines and chemokines and enhanced the IL-10 production in vivo and in vitro.

5. Conclusion

CRTH2 antagonism with CT-133 strikingly alleviated CS-induced acute lung injury through inhibition of inappropriate pulmonary trafficking of macrophages and neutrophils, reduction of pulmonary vascular permeability, amelioration of pro-inflammatory cytokines and chemokine production, and augmentation of IL-10 production. We found for the first time that CRTH2 receptor could be a new potential therapeutic target for appropriate therapy of CS-induced lung injury.

Acknowledgment

This work is supported by National Natural Science Foundation of China (no. 81372046, 81571928, 81470214, 81200022, and 81270067); and Science and Technology Department of Zhejiang Province (LGF18H150002).

Conflict of interest

All authors declare that they have no conflict of interest.

Author's contributions

M.H., C.X., and M.Y., performed the research and wrote the manuscript. Z.Q., and W.J., and W.X., analyzed the data. L.M., and T.L., prepared the figs. W.F., and W.X., designed and supervised the manuscript.

References

[1] B.T. Thompson, R.C. Chambers, K.D. Liu, Acute respiratory distress syndrome, N. Engl. J. Med. 377 (6) (2017) 562–572, https://doi.org/10.1056/NEJMra1608077.
[2] G. Bellani, J.G. Laffey, T. Pham, E. Fan, L. Brochard, A. Esteban, L. Gattinoni, F. Van Haren, A. Larsson, D.F. McAuley, Epidemiology, patterns of care, and mortality for patients with acute respiratory distress syndrome in intensive care units in 50 countries, JAMA 315 (8) (2016) 788–800, https://doi.org/10.1001/jama.2016.0291.
[3] M. Hussain, C. Xu, M. Ahmad, A. Majeed, M. Lu, X. Wu, L. Tang, X. Wu, Acute respiratory distress syndrome: bench-to-bedside approaches to improve drug development, Clin. Pharmacol. Ther. 104 (3) (2018) 484–494, https://doi.org/10.1002/cpt.1034.
[4] J. Lee, V. Taneja, R. Vassallo, Cigarette smoking and inflammation: cellular and molecular mechanisms, J. Dent. Res. 91 (2) (2012) 142–149, https://doi.org/10.1177/0022034511421200.
[5] C.S. Calfee, M.A. Matthay, M.D. Eisner, N. Benowitz, M. Call, J.-F. Pittet, M.J. Cohen, Active and passive cigarette smoking and acute lung injury after severe blunt trauma, Am. J. Respir. Crit. Care Med. 183 (12) (2011) 1660–1665, https://doi.org/10.1164/rccm.201011-1802OC.
[6] C.S. Calfee, M.A. Matthay, K.N. Kangelaris, E.D. Siew, D.R. Janz, G.R. Bernard, A.K. May, P. Jacob, C. Havel, N.L. Benowitz, Cigarette smoke exposure and the acute respiratory distress syndrome, Crit. Care Med. 43 (9) (2015) 1790, https://doi.org/10.1097/CCM.0000000000001089.
[7] S.J. Hsieh, H. Zhuo, N.L. Benowitz, B.T. Thompson, K.D. Liu, M.A. Matthay, C.S. Calfee, N.A. Network, Prevalence and impact of active and passive cigarette smoking in acute respiratory distress syndrome, Crit. Care Med. 42 (9) (2014), https://doi.org/10.1097/CCM.0000000000000418.
[8] W. MacNee, B. Wiggs, A.S. Belzberg, J.C. Hogg, The effect of cigarette smoking on neutrophil kinetics in human lungs, N. Engl. J. Med. 321 (14) (1989) 924–928, https://doi.org/10.1056/NEJM198910053211402.
[9] L. Arcavi, N.L. Benowitz, Cigarette smoking and infection, Arch. Intern. Med. 164 (20) (2004) 2206–2216, https://doi.org/10.1001/archinte.164.20.2206.
[10] G. Mason, J. Uszler, R. Effros, E. Reid, Rapidly reversible alterations of pulmonary epithelial permeability induced by smoking, Chest 83 (1) (1983) 6–11, https://doi.org/10.1378/chest.83.1.6.
[11] X. Li, I. Rahman, K. Donaldson, W. MacNee, Mechanisms of cigarette smoke induced increased airspace permeability, Thorax 51 (5) (1996) 465–471.
[12] D.K. Bhalla, F. Hirata, A.K. Rishi, C.G. Gairola, Cigarette smoke, inflammation, and lung injury: a mechanistic perspective, J. Toxicol. Environ. Health Part B 12 (1) (2009) 45–64, https://doi.org/10.1080/10937400802545094.
[13] K. Jandl, A. Heinemann, The therapeutic potential of CRTH2/DP2 beyond allergy and asthma, Prostaglandins Other Lipid Mediat. 113 (11) (2017) 42–48, https://doi.org/10.1016/j.prostaglandins.2017.08.006.
[14] A. Small-Howard, H. Turner, Exposure to tobacco-derived materials induces overproduction of secreted proteinases in mast cells, Toxicol. Appl. Pharmacol. 204 (2) (2005) 152–163, https://doi.org/10.1016/j.taap.2004.09.003.
[15] W. Grashoff, J.K. Sont, P.J. Sterk, P.S. Hiemstra, W. De Boer, J. Stolk, J. Han, J. Van Krieken, Chronic obstructive pulmonary disease: role of bronchiolar mast cells and macrophages, Am. J. Pathol. 151 (6) (1997) 1785.
[16] R. Lewis, N. Soter, P. Diamond, K. Austen, J. Oates, L.N. Roberts, Prostaglandin D2 generation after activation of rat and human mast cells with anti-IgE, J. Immunol. 129 (4) (1982) 1627–1631.
[17] P.S. Thomas, R.E. Schreck, S.C. Lazarus, Tobacco smoke releases performed mediators from canine mast cells and modulates prostaglandin production, Am. J. Phys. Lung Cell. Mol. Phys. 263 (1) (1992) L67–L72.
[18] B. Phillips, E. Veljkovic, M.J. Peck, A. Buettner, A. Elamin, E. Guedj, G. Vuillaume, N.V. Ivanov, F. Martin, S. Boué, A 7-month cigarette smoke inhalation study in C57BL/6 mice demonstrates reduced lung inflammation and emphysema following smoking cessation or aerosol exposure from a prototypic modified risk tobacco product, Food Chem. Toxicol. 80 (2015) 328–345, https://doi.org/10.1016/j.fct.2015.03.009.
[19] J.L. Hong, L.Y. Lee, Cigarette smoke-induced bronchoconstriction: causative agents and role of thromboxane receptors, J. Appl. Physiol. 81 (5) (1996) 2053–2059, https://doi.org/10.1152/jappl.1996.81.5.2053.
[20] N. Snell, M. Foster, J. Vestbo, Efficacy and safety of AZD1981, a CRTH2 receptor antagonist, in patients with moderate to severe COPD, Respir. Med. 107 (11) (2013) 1722–1730, https://doi.org/10.1016/j.rmed.2013.06.006.
[21] E. Csanky, R. Rühl, B. Scholtz, A. Vasko, L. Takacs, W.M. Hempel, Lipid metabolite levels of prostaglandin D2 and eicosapentaenoic acid recovered from bronchoalveolar lavage fluid correlate with lung function of chronic obstructive pulmonary disease patients and controls, Electrophoresis 30 (7) (2009) 1228–1234, https://doi.org/10.1002/elps.200800722.
[22] K. Jandl, E. Stacher, Z. Bálint, E.M. Sturm, J. Maric, M. Peinhaupt, P. Luschnig, I. Aringer, A. Fauland, V. Konya, Activated prostaglandin D2 receptors on macrophages enhance neutrophil recruitment into the lung, J. Allergy Clin. Immunol. 137 (3) (2016) 833–843, https://doi.org/10.1016/j.jaci.2015.11.012.
[23] K.J. Stebbins, A.R. Broadhead, C.S. Baccei, J.M. Scott, Y.P. Truong, H. Coate, N.S. Stock, A.M. Santini, P. Fagan, P. Prodanovich, Pharmacological blockade of the DP2 receptor inhibits cigarette smoke-induced inflammation, mucus cell metaplasia, and epithelial hyperplasia in the mouse lung, J. Pharmacol. Exp. Ther. 332 (3) (2010) 764–775, https://doi.org/10.1124/jpet.109.161919.
[24] C. Sargent, S. Stinson, J. Schmidt, I. Dougall, R. Bonnert, S. Paine, M. Saunders, M. Foster, The effect of a selective CRTh2 antagonist on tobacco smoke (TS) induced airway inflammation and remodelling in the mouse, Br. J. Pharmacol. 7 (2009).
[25] S. Suzuki, M. Ishii, T. Asami, H. Namkoong, K. Yagi, T. Asakura, H. Kamata, S. Tasaka, S. Kagawa, T. Kamo, Critical role of the prostaglandin D2 receptor CRTH2 in acute lung injury caused by lipopolysaccharide (LPS)-induced shock in mice, C105. Respiratory failure: mechanistic insights from lung injury models, American Thoracic Society (2016) A6285.
[26] D. Guo, The in vivo profile of CT133, a potent, well tolerated, and selective CRTH2

antagonist for the treatment of allergic asthma and rhinitis, J. Allergy Clin. Immunol. 135 (2) (2015) AB3, https://doi.org/10.1016/j.jaci.2014.12.946.
[27] W. Huvenne, C.A. Pérez-Novo, L. Derycke, N. De Ruyck, O. Krysko, T. Maes, N. Pauwels, L. Robays, K.R. Bracke, G. Joos, Different regulation of cigarette smoke induced inflammation in upper versus lower airways, Respir. Res. 11 (1) (2010) 100, https://doi.org/10.1186/1465-9921-11-100.
[28] X. Zhang, R. Zhuang, H. Wu, J. Chen, F. Wang, G. Li, C. Wu, A novel role of endocan in alleviating LPS-induced acute lung injury, Life Sci. 202 (2018) 89–97, https://doi.org/10.1016/j.lfs.2018.04.005.
[29] W. Shi, C. Xu, M. Hussain, F. Wu, M. Lu, X. Wu, L. Tang, X. Wu, J. Wu, Inhibition of myosin light-chain kinase enhances the clearance of lipopolysaccharide-induced lung inflammation possibly by accelerating neutrophil apoptosis, Shock 48 (3) (2017) 377–386, https://doi.org/10.1097/SHK.0000000000000863.
[31] M. Ishii, K. Asano, H. Namkoong, S. Tasaka, K. Mizoguchi, T. Asami, H. Kamata, Y. Kimizuka, H. Fujiwara, Y. Funatsu, CRTH2 is a critical regulator of neutrophil migration and resistance to polymicrobial sepsis, J. Immunol. 1102330 (2012), https://doi.org/10.4049/jimmunol.1102330.
[32] Q. Lu, P. Sakhatskyy, K. Grinnell, J. Newton, M. Ortiz, Y. Wang, J. Sanchez-Esteban, E.O. Harrington, S. Rounds, Cigarette smoke causes lung vascular barrier dysfunction via oxidative stress-mediated inhibition of RhoA and focal adhesion kinase, Am. J. Phys. Lung Cell. Mol. Phys. 301 (6) (2011) L847–L857, https://doi.org/10.1152/ajplung.00178.2011.
[33] J.Q. Davies, S. Gordon, Isolation and Culture of Murine Macrophages, Basic Cell Culture Protocols, Springer, 2005, pp. 91–103, https://doi.org/10.1385/1-59259-838-2:091.
[34] M. Sopori, Effects of cigarette smoke on the immune system, Nat. Rev. Immunol. 2 (5) (2002) 372, https://doi.org/10.1038/nri803.
[35] A. D'hulst, K. Vermaelen, G. Brusselle, G. Joos, R. Pauwels, Time course of cigarette smoke-induced pulmonary inflammation in mice, Eur. Respir. J. 26 (2) (2005) 204–213, https://doi.org/10.1183/09031936.05.00095204.
[36] T.E. King Jr., D. Savici, P.A. Campbell, Phagocytosis and killing of *Listeria monocytogenes* by alveolar macrophages: smokers versus nonsmokers, J. Infect. Dis. 158 (6) (1988) 1309–1316.
[37] C.S. Berenson, M.A. Garlipp, L.J. Grove, J. Maloney, S. Sethi, Impaired phagocytosis of nontypeable Haemophilus influenzae by human alveolar macrophages in chronic obstructive pulmonary disease, J. Infect. Dis. 194 (10) (2006) 1375–1384.
[38] B. Zappacosta, S. Persichilli, A. Minucci, E.D. Stasio, P. Carlino, G. Pagliari, B. Giardina, P.D. Sole, Effect of aqueous cigarette smoke extract on the chemiluminescence kinetics of polymorphonuclear leukocytes and on their glycolytic and phagocytic activity, Lumin. J. Biol. Chem. Lumin. 16 (5) (2001) 315–319, https://doi.org/10.1002/bio.661.
[39] D. Borgas, E. Chambers, J. Newton, J. Ko, S. Rivera, S. Rounds, Q. Lu, Cigarette smoke disrupted lung endothelial barrier integrity and increased susceptibility to acute lung injury via histone deacetylase 6, Am. J. Respir. Cell Mol. Biol. 54 (5) (2016) 683–696, https://doi.org/10.1165/rcmb.2015-0149OC.
[40] A.R. Burns, S.P. Hosford, L.A. Dunn, D.C. Walker, J.C. Hogg, Respiratory epithelial permeability after cigarette smoke exposure in Guinea pigs, J. Appl. Physiol. 66 (5) (1989) 2109–2116, https://doi.org/10.1152/jappl.1989.66.5.2109.
[41] M. Shichijo, H. Sugimoto, K. Nagao, H. Inbe, J.A. Encinas, K. Takeshita, K.B. Bacon, F. Gantner, Chemoattractant receptor-homologous molecule expressed on Th2 cells activation in vivo increases blood leukocyte counts and its blockade abrogates 13, 14-dihydro-15-keto-prostaglandin D2-induced eosinophilia in rats, J. Pharmacol. Exp. Ther. 307 (2) (2003) 518–525, https://doi.org/10.1124/jpet.103.055442.
[42] K.J. Stebbins, A.R. Broadhead, L.D. Correa, J.M. Scott, Y.P. Truong, B.A. Stearns, J.H. Hutchinson, P. Prasit, J.F. Evans, D.S. Lorrain, Therapeutic efficacy of AM156, a novel prostanoid DP2 receptor antagonist, in murine models of allergic rhinitis and house dust mite-induced pulmonary inflammation, Eur. J. Pharmacol. 638 (1–3) (2010) 142–149, https://doi.org/10.1016/j.ejphar.2010.04.031.
[43] J.K. Quint, J.A. Wedzicha, The neutrophil in chronic obstructive pulmonary disease, J. Allergy Clin. Immunol. 119 (5) (2007) 1065–1071, https://doi.org/10.1016/j.jaci.2006.12.640.
[44] R. Dhami, B. Gilks, C. Xie, K. Zay, J.L. Wright, A. Churg, Acute cigarette smoke–induced connective tissue breakdown is mediated by neutrophils and prevented by α 1-antitrypsin, Am. J. Respir. Cell Mol. Biol. 22 (2) (2000) 244–252, https://doi.org/10.1165/ajrcmb.22.2.3809.
[45] K.H. Jung, H. Beak, S. Park, D. Shin, J. Jung, S. Park, J. Kim, H. Bae, The therapeutic effects of tuberostemonine against cigarette smoke-induced acute lung inflammation in mice, Eur. J. Pharmacol. 774 (2016) 80–86, https://doi.org/10.1016/j.ejphar.2016.02.006.
[46] J.W. Lee, N.R. Shin, J.W. Park, S.-Y. Park, O.K. Kwon, H.S. Lee, J.H. Kim, H.J. Lee, J. Lee, Z.Y. Zhang, *Callicarpa japonica* Thunb. attenuates cigarette smoke-induced neutrophil inflammation and mucus secretion, J. Ethnopharmacol. 175 (2015) 1–8, https://doi.org/10.1016/j.jep.2015.08.056.
[47] A. Churg, K. Zay, S. Shay, C. Xie, S.D. Shapiro, R. Hendricks, J.L. Wright, Acute cigarette smoke–induced connective tissue breakdown requires both neutrophils and macrophage metalloelastase in mice, Am. J. Respir. Cell Mol. Biol. 27 (3) (2002) 368–374, https://doi.org/10.1165/rcmb.4791.
[48] D. Lim, W. Kim, C. Lee, H. Bae, J. Kim, Macrophage depletion protects against cigarette smoke-induced inflammatory response in the mouse colon and lung, Front. Physiol. 9 (2018) 47, https://doi.org/10.3389/fphys.2018.00047.
[49] A. Churg, J. Dai, H. Tai, C. Xie, J.L. Wright, Tumor necrosis factor-α is central to acute cigarette smoke–induced inflammation and connective tissue breakdown, Am. J. Respir. Crit. Care Med. 166 (6) (2002) 849–854, https://doi.org/10.1164/rccm.200202-097OC.
[50] L. Demirjian, R.T. Abboud, H. Li, V. Duronio, Acute effect of cigarette smoke on TNF-α release by macrophages mediated through the erk1/2 pathway, Biochim. Biophys. Acta (BBA) - Mol. Basis Dis. 1762 (6) (2006) 592–597, https://doi.org/10.1016/j.bbadis.2006.04.004.
[51] U. Lappalainen, J.A. Whitsett, S.E. Wert, J.W. Tichelaar, K. Bry, Interleukin-1β causes pulmonary inflammation, emphysema, and airway remodeling in the adult murine lung, Am. J. Respir. Cell Mol. Biol. 32 (4) (2005) 311–318, https://doi.org/10.1165/rcmb.2004-0309OC.
[52] S. Mukhopadhyay, J.R. Hoidal, T.K. Mukherjee, Role of TNFα in pulmonary pathophysiology, Respir. Res. 7 (1) (2006) 125, https://doi.org/10.1186/1465-9921-7-125.
[53] G.Y. Kim, J.W. Lee, H.-C. Ryu, J.D. Wei, C.M. Seong, J.H. Kim, Proinflammatory cytokine IL-1β stimulates IL-8 synthesis in mast cells via a leukotriene B4 receptor 2-linked pathway, contributing to angiogenesis, J. Immunol. (2010), https://doi.org/10.4049/jimmunol.0901735.
[54] R.M. Strieter, S.L. Kunkel, Acute lung injury: the role of cytokines in the elicitation of neutrophils, J. Investig. Med. 42 (4) (1994) 640–651.
[55] S. Chollet-Martin, B. Jourdain, C. Gibert, C. Elbim, J. Chastre, M.A. Gougerot-Pocidalo, Interactions between neutrophils and cytokines in blood and alveolar spaces during ARDS, Am. J. Respir. Crit. Care Med. 154 (3) (1996) 594–601, https://doi.org/10.1164/ajrccm.154.3.8810592.
[56] M. Singer, P.J. Sansonetti, IL-8 is a key chemokine regulating neutrophil recruitment in a new mouse model of Shigella-induced colitis, J. Immunol. 173 (6) (2004) 4197–4206, https://doi.org/10.4049/jimmunol.173.6.4197.
[57] M. Hammond, G.R. Lapointe, P.H. Feucht, S. Hilt, C.A. Gallegos, C.A. Gordon, M.A. Giedlin, G. Mullenbach, P. Tekamp-Olson, IL-8 induces neutrophil chemotaxis predominantly via type I IL-8 receptors, J. Immunol. 155 (3) (1995) 1428–1433.
[58] C.A. Lerner, W. Lei, I.K. Sundar, I. Rahman, Genetic ablation of CXCR2 protects against cigarette smoke-induced lung inflammation and injury, Front. Pharmacol. 7 (2016) 391, https://doi.org/10.3389/fphar.2016.00391.
[59] G.J. Tang, H.Y. Wang, J.Y. Wang, C.C. Lee, H.W. Tseng, Y.L. Wu, S.K. Shyue, T.S. Lee, Y.R. Kou, Novel role of AMP-activated protein kinase signaling in cigarette smoke induction of IL-8 in human lung epithelial cells and lung inflammation in mice, Free Radic. Biol. Med. 50 (11) (2011) 1492–1502, https://doi.org/10.1016/j.freeradbiomed.2011.02.030.
[60] V. Dubar, P. Gosset, C. Aerts, C. Voisin, B. Wallaert, A.B. Tonnel, In vitro acute effects of tobacco smoke on tumor necrosis factor a and interleukin-6 production by alveolar macrophages, Exp. Lung Res. 19 (3) (1993) 345–359.
[61] W. Kuschner, A. D'Alessandro, H. Wong, P. Blanc, Dose-dependent cigarette smoking-related inflammatory responses in healthy adults, Eur. Respir. J. 9 (10) (1996) 1989–1994, https://doi.org/10.1183/09031936.96.09101989.
[62] M. Ryder, M. Saghizadeh, Y. Ding, N. Nguyen, A. Soskolne, Effects of tobacco smoke on the secretion of interleukin-1β, tumor necrosis factor-α, and transforming growth factor-β from peripheral blood mononuclear cells, Oral Microbiol. Immunol. 17 (6) (2002) 331–336, https://doi.org/10.1034/j.1399-302X.2002.170601.x.
[63] A. Churg, R.D. Wang, H. Tai, X. Wang, C. Xie, J. Dai, S.D. Shapiro, J.L. Wright, Macrophage metalloelastase mediates acute cigarette smoke–induced inflammation via tumor necrosis factor-α release, Am. J. Respir. Crit. Care Med. 167 (8) (2003) 1083–1089, https://doi.org/10.1164/rccm.200212-1396OC.
[64] J.W. Lee, H.A. Park, O.K. Kwon, Y.G. Jang, J.Y. Kim, B.K. Choi, H.J. Lee, S. Lee, J.H. Paik, R. Oh, Asiatic acid inhibits pulmonary inflammation induced by cigarette smoke, Int. Immunopharmacol. 39 (2016) 208–217, https://doi.org/10.1016/j.intimp.2016.07.010.
[65] J. Ma, H. Xu, J. Wu, C. Qu, F. Sun, S. Xu, Linalool inhibits cigarette smoke-induced lung inflammation by inhibiting NF-κB activation, Int. Immunopharmacol. 29 (2) (2015) 708–713, https://doi.org/10.1016/j.intimp.2015.09.005.
[66] S. Guan, Y. Zheng, X. Yu, W. Li, B. Han, J. Lu, Ellagic acid protects against LPS-induced acute lung injury through inhibition of nuclear factor kappa B, proinflammatory cytokines and enhancement of interleukin-10, Food Agric. Immunol. 28 (6) (2017) 1347–1361, https://doi.org/10.1080/09540105.2017.1339670.
[67] C.L. Wu, L.Y. Lin, J.S. Yang, M.C. Chan, C.M. Hsueh, Attenuation of lipopolysaccharide-induced acute lung injury by treatment with IL-10, Respirology 14 (4) (2009) 511–521, https://doi.org/10.1111/j.1440-1843.2009.01516.x.